Title

Non-neural surface ectodermal rosette formation and F-actin dynamics drive mammalian neural tube closure

Journal

Biochemical and Biophysical Research Communications, 526(3)

ISSN

0006-291X

Authors

Zhou, Chengji J

Ji, Yu

Reynolds, Kurt

et al.

Publication Date

2020-06-01

DOI

10.1016/j.bbrc.2020.03.138

Peer reviewed

HHS Public Access

Author manuscript

Biochem Biophys Res Commun. Author manuscript; available in PMC 2021 June 04.

Published in final edited form as:

Biochem Biophys Res Commun. 2020 June 04; 526(3): 647–653. doi:10.1016/j.bbrc.2020.03.138.

Non-neural surface ectodermal rosette formation and F-actin dynamics drive mammalian neural tube closure

Chengji J. Zhou[a,b,*], **Yu Ji**[a,b], **Kurt Reynolds**[a,b], **Moira McMahon**[a], **Michael Garland**[a,b], **Shuwen Zhang**[a,b], **Bo Sun**[a,b], **Ran Gu**[a,b], **Mohammad Islam**[a], **Yue Liu**[a], **Tianyu Zhao**[a], **Grace Hsu**[c], **Janet Iwasa**[c]

[a]Institute for Pediatric Regenerative Medicine, Shriners Hospitals for Children & University of California at Davis, School of Medicine, Sacramento, CA 95817, USA.

[b]Department of Biochemistry and Molecular Medicine, School of Medicine, University of California at Davis, Sacramento, CA 95817, USA.

[c]Department of Biochemistry, University of Utah, Salt Lake City, UT 84112, USA.

Abstract

The mechanisms underlying mammalian neural tube closure remain poorly understood. We report a unique cellular process involving multicellular rosette formation, convergent cellular protrusions, and F-actin cable network of the non-neural surface ectodermal cells encircling the closure site of the posterior neural pore, which are demonstrated by scanning electron microscopy and genetic fate mapping analyses during mouse spinal neurulation. These unique cellular structures are severely disrupted in the surface ectodermal transcription factor Grhl3 mutants that exhibit fully penetrant spina bifida. We propose a novel model of mammalian neural tube closure driven by surface ectodermal dynamics, which is computationally visualized.

Graphical Abstract

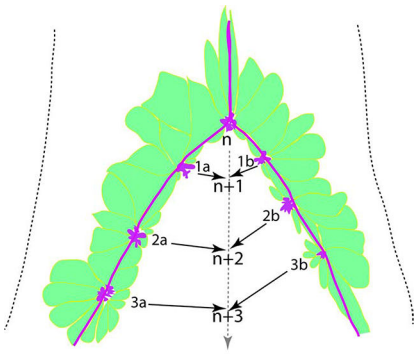

*Correspondence author. C.J. Zhou, 2425 Stockton Blvd., Room-602B, Sacramento, CA 95817; Phone: 916-453-2268; cjzhou@ucdavis.edu.

Keywords

Non-neural surface ectodermal cells; multicellular rosette formation; convergent F-actin protrusions and cable network; posterior neural pore (PNP); *Grhl3-KO* mice; computational visual modeling

1. Introduction

The neural tube is the embryonic precursor structure of the brain and spinal cord. During mammalian neurulation, neural tube closure initiates at the border region of the future brain and spinal cord, and the closure spreads rapidly towards both anterior and posterior directions to seal up the brain and spinal cord [1,2]. Defective closure of the neural tube may cause neural tube closure defects (NTDs), which is among the commonest and severest structural birth defects in humans [3–6]. Among various anatomically distinct NTDs, spina bifida, resulted from defective caudal neural tube closure, is the commonest NTDs affecting numerous liveborn infants [7,8]. Mutant mice have been long and widely used to address the cause and prevention of human neural tube defects [9–14]. Thus, understanding the basic mechanisms of normal and defective neural tube closure, particularly, the spinal neurulation in the mouse model, is both scientifically and clinically significant.

The neural tube arises from the neural plate flanked by the non-neural surface ectoderm. Numerous studies focused on the apical constriction of the neuroepithelial cells and neural plate bending [15–17], while little is known about the role of the non-neural surface ectodermal cells in neural tube closure. It has been long known that cellular protrusions (referred as ruffles or lamellipodia) present at the dorsal tips of mouse neural folds [18,19]. A recent study shows that these cellular protrusions are regulated by small GTPase Rac1 and may be extended from the surface ectodermal cells during mouse spinal neurulation [20]. Nevertheless, it remains unknown how these cellular protrusions are generated and whether these cellular protrusions and related surface ectodermal cells play an active role in neural tube closure.

In this study, we found unique cellular structures of the non-neural surface ectodermal cells that form multicellular rosette-like structures and convergent F-actin protrusions and cable network encircling the closure site during posterior neural tube closure, which are severely disrupted in the mutant mouse models with fully penetrant spina bifida. These results provide evidence for a novel neural tube closure model driven by the non-neural surface ectodermal cell dynamics, which is computationally visualized.

2. Materials and methods

2.1. Animals

The *Grhl3*^{Cre} knock-in mouse line [21] was acquired through the Mutant Mouse Resource & Research Centers (MMRRC) at UC Davis. *Rosa26-mT/mG* reporter mice [22] were acquired through the Jackson Laboratory. All research procedures using laboratory mice were approved by UC Davis Animal Care and Use Committee and conform to NIH

guidelines. Pregnant, timed mated mice were euthanized prior to cesarean section. The noon of the conception day was designated as E0.5.

2.2. Scanning electron microscopy (SEM)

SEM was carried out as previously described [23]. Briefly, mouse embryos were fixed in 2.5% glutaraldehyde and 2% paraformaldehyde (PFA) in PBS and dehydrated in a graded ethanol (200 proof) series. Hexamethyldisilazane (HMDS) was used for the final drying of samples. The treated embryos were mounted on aluminum stubs and then sputter coated with gold (Pelco Auto Sputter Coater, Ted Pella) for scanning electron microscopy (Phillips XL30 TMP, F.E.I. Company, Hillsboro, OR, USA).

2.3. Wholemount immunofluorescence, F-actin labeling, and confocal microscopy

Mouse embryos were dissected into ice-cold PBS and fixed in 4% PFA in PBS overnight in the cold room. Wholemount immunofluorescence was performed according to standard protocols with slightly modifications. Briefly, fixed embryos were washed three times for 30 minutes each time in PBS with 0.1% TritonX-100, blocked in PBS with 0.1% TritonX-100 and 5% donkey serum for 2 hours, incubated in diluted primary antibodies in PBS with 0.1% TritonX-100 and 1% donkey serum overnight in cold room with gentle rocking, washed three times for 1 hour each time in PBS with 0.1% TritonX-100, incubated in diluted secondary antibodies in PBS 0.1% TritonX-100 and 1% donkey serum for 4 hours, washed three times for 30 minutes each time in PBS with 0.1% TritonX-100 by gentle rocking, counter-stained in PBS with 1μg/ml DAPI for 20 minutes with gentle rocking. The antibodies and dilutions were as following: Rabbit anti ß-tubulin (1:100, Cell Signaling), Rat anti-E-cadherin ((1:300, EMD Millipore), and Alexa 488 donkey anti-rabbit or rat IgG (1:200, Invitrogen). Alexa Fluor Phalloidin (1:100, Invitrogen) was used for F-actin staining. The stained embryos were transferred to a Petri dish with 4% agarose (for positioning embryos) filled with PBS for confocal imaging (Nikon A1 confocal laser microscope with NIS-Elements C software).

2.4. Dynamic visual modeling of neural tube closure at single-cell resolution

Using our scanning electron microscopy and immunofluorescence confocal micrographs as references, a dynamic closure model of the mouse caudal neural tube was created by a digital sculpting software Pixologic ZBrush. This 3D model was imported into a computer animation & modeling software Autodesk Maya and a custom animation rig was developed to visualize the dynamic closure process at single-cell resolution. In addition, convergent F-actin protrusions and F-actin cables were modeled and rigged separately in Maya. This dynamic model was rendered into a series of images from Maya and imported into Adobe After Effects for compositing and creation of the final video.

3. Results

3.1. Scanning electron microscopy reveals multicellular structures of non-neural surface ectodermal cells during posterior neural tube closure

Using scanning electron microscopy (SEM), we found a large rosette-shaped multicellular structure that is formed by surface ectodermal cells and is converged with clustered cellular

protrusions at the leading midline fusion site of the mouse posterior neural pore (PNP) around embryonic day (E) 9.5 (around 24-somite stage (ss24)) (Fig. 1A and E). This large midline rosette has partial opening with the pending closure gap towards the posterior direction. Around ss28 (Fig. 1B and F), two large midline rosettes with convergent protrusions are found at both anterior and posterior leading fusion sites, consisting of 10 to 14 visible cells (no. 1 & no. 7 in Fig. 1F). Between these two midline rosettes, there are 5 paired partial rosettes/protrusions (no. 2 to no. 6 in Fig. 1F) located at the opposing sides of the pending closure gap of the PNP. Along the pending closure edge, one or two visible and elongated cells contribute to two adjacent rosettes and protrusions. Around ss32 (Fig. 1C and G), the last two midline rosettes/protrusions (labeled no. 3 and no. 4 in Fig. 1G, presumably equivalent to the same numbers for the regions with the largest pending closing gap in Fig. 1F) merged through a shortened surface ectodermal cell on each side of the final midline epithelial fusion site. These SEM observations strongly suggest that each rosette-forming cell generates cellular protrusions that are intermingled and converged together to mediate surface ectodermal cell fusion at the leading midline closure site, to seal up the pending closure gap, and to complete the final midline closure process. These observations indicate that the surface ectodermal rosette formation and convergent cellular protrusions may play a previously unrecognized active role in neural tube closure.

3.2. The rosette formation and convergent F-actin protrusions are disrupted in the surface ectodermal Grhl3 mutants with fully penetrant spina bifida

To demonstrate this speculation, we examined these unique cellular processes in the surface ectodermal mutant mice that exhibit fully penetrant spinal NTDs. Indeed, the surface ectodermal rosette formation and convergent protrusions are severely disrupted in the mutant PNPs of *Grhl3*$^{Cre/Cre}$ (*Grhl3-KO*) [21] mouse embryos at E9.5 (Fig. 2). The grainyhead-like transcription factor Grhl3 is predominantly expressed in the surface ectodermal cells and is required for epidermal development and neural tube closure (particularly, spina bifida) [24–27]. In addition to the missing midline rosette and protrusions at the fusion site, small rosettes centered with visible protrusions are abnormally located away from the closure edge in the *Grhl3-KO* PNPs (Fig. 2A and B). Together, these results demonstrate that a local signaling cascade mediated by transcription factor Grhl3 is required for the surface ectodermal rosette formation and convergent cellular protrusions to promote PNP closure.

3.3. Genetic fate mapping and immunofluorescence confocal microscopy demonstrate the surface ectodermal nature of the rosette-forming cells that generate the F-actin protrusions and cable network during posterior neural tube closure

To further demonstrate the role of surface ectodermal cells and the nature of the cellular protrusions in neural tube closure, we conducted genetic fate mapping by crossing *Grhl3*$^{Cre/+}$ mice with the Cre reporter *Rosa*$^{mT/mG}$ mice [22], in combination with F-actin labeling by fluorescence-conjugated phalloidin (Fig. 3). We found that the rosette-forming cells are Grhl3-expressing lineage cells that wrap the opposing dorsal tips of the pending closing PNP (Fig. 3A and A1). These cells generate the F-actin-based cellular protrusions (Fig. 3B and B1), evident by the complete overlapping of the fate-mapped membrane EGFP and F-actin labeling (Fig. 3C and C1). At the leading closure site, the EGFP/F-actin colabeled cellular protrusions merge at the midline connecting the opposing tips of the

dorsal PNP (Fig. 3A2–C2). At the newly closed dorsal midline, the EGFP-labeled cells attached or fused to each other, bridging the dorsal neuroepithelial cells on each side of the PNP (Fig. 3A3–C3). Notably, the rosette-forming cells also generate a large and tangentially oriented F-actin cable network with a cable running anteriorly from the leading fusing site along the recently closed midline, and two cables separated from the leading fusion site running posteriorly along the edges of the pending closing gaps (Fig. 3B,B3,C,C3). The posteriorly running F-actin cables have recently been shown to form a cable ring connecting cellular protrusions around the pending closure site and to play a role in biomechanical coupling for PNP closure at late somite stages [28]. The surface ectodermal nature of these rosette-forming cells wrapping along the dorsal edges of the PNP is also demonstrated by the immunolabeling of ß-tubulin or the surface ectoderm adherens junction marker E-cadherin (Fig. 4A and B). Although E-cadherin immunolabeling also shows some signals in the neuroepithelial cells, it has been used to support that the non-neural surface ectoderm wraps around neural ectoderm right before the neural folds meet during mouse cranial neural tube closure [29]. Our genetic fate mapping and immunolabeling results provide conclusive evidence for the non-neural surface ectodermal nature of the rosette-forming cells (Fig. 4C) that wrap around the pending closure tips and fuse at the dorsal midline by merging the convergent cellular protrusions during posterior neural tube closure.

3.4. Computational visual model of the dynamic neural tube closure process driven by non-neural surface ectodermal cells and F-actin dynamics

Based our SEM, genetic fate mapping, and immunolabeling results, we propose a dynamic model of PNP closure driven by surface ectodermal rosette formation and F-actin protrusion/cable network (Fig. 4D & Movie 1). Each rosette-forming cell generates polarized F-actin protrusion that converges at the center of the rosette to form a large cluster of F-actin protrusions. There are one or two elongated cells running along the F-actin cable. Both ends of these cells generate F-actin protrusions connecting two adjacent rosettes. Thus, the convergent protrusions of the adjacent rosettes generate the force to tighten the F-actin cables between them and to pull the paired rosettes toward the midline. When the first pair (next to the leading fusion site) of rosette protrusions meet and fuse at the midline, a transiently existing full rosette will form at the midline, resulting in one-cell length closure. Sequentially, it will start the next full rosette formation when the next paired rosettes meet at the midline, and so on, advancing the PNP closure (Fig. 4D & Movie 1).

4. Discussion

The current study revealed novel mechanisms of mouse neural tube closure driven by the non-neural surface ectoderm cells. Neural tube closure involves dynamic morphogenetic movements, such as convergent extension, neural plate bending, and apical constriction of neuroepithelial cells. However, the role of the non-neural surface ectodermal cells in neural tube closure remained poorly understood until recently. Meanwhile, the dynamics of mammalian neural tube closure has been understudied due to the challenge of live imaging experiments for in utero development [30]. The Niswander group has pioneered ex vivo live imaging of mouse neurulation and revealed several important findings in cranial neural tube closure, including the filopodia- and lamellipodia-like cellular projections from the non-

neural ectoderm and membrane shuttling during cranial neural tube closure [29,31,32]. These findings suggest an active role of the non-neural surface ectodermal cells in mammalian neural tube closure. However, it remains unknown how these cellular projections are generated and whether they are essential for cranial neural tube closure. It also remains unclear if similar cellular dynamics may occur during spinal neurulation, which should be addressed in future live imaging studies.

Our SEM, genetic fate-mapping, and gene-targeting results clearly demonstrate that the non-neural surface ectodermal cells form rosette-like multicellular structures that generate the F-actin-based convergent protrusions for dorsal midline fusion during spinal neurulation, which are disrupted in the surface ectodermal mutants of *Grhl3-KO* mice that exhibit fully penetrant spina bifida [24]. The surface ectodermal role of Grhl3 in PNP closure is further demonstrated by its expression timing and conditional ablation of Grhl3 in the neuroepithelium using $Nkx1–2^{Cre}$, which generated no spina bifida [33]. Together, these results demonstrate that Grhl3 is required for non-neural surface ectodermal rosette formation and convergent cellular protrusions to fuse the dorsal midline during PNP closure. Intriguingly, conditional ablation of Grhl3 in the hindgut using $Sox17^{Cre}$ generated partial penetrant spina bifida, supporting the hypothesis that diminished Grhl3 expression in the hindgut maybe the cause of spina bifida in the *curly tail* mice with a hypomorphic *Grhl3* allele [33]. Increased expression of Grhl3 can rescue spina bifida in the *curly tail* mice [27], but transgenic overexpression of Grhl3 also causes spina bifida [34]. It would be important to examine whether non-neural ectodermal rosette formation and F-actin dynamics are intact or disrupted in $Grhl3^{fl/fl};Sox17^{Cre}$ (hindgut ablation), *curly tail* (hypomorphic *Grhl3*), or homozygous *TgGrhl3* (gain-of-function) mouse embryos during spinal neurulation.

We have previously demonstrated that canonical Wnt/beta-catenin signaling regulates transcription factors Pax3 and Cdx2 to promote spinal neural tube closure in mice [35]. Nevertheless, it remains unknown if Pax3 and Cdx2 also play a role in the surface ectodermal dynamics during neural tube closure. Grhl3 has been suggested to act downstream of canonical Wnt signaling to specify the neural plate border cells during mouse neural tube closure [36]. Therefore, it is highly possible that Wnt/beta-catenin signaling also regulates Grhl3 to promote surface ectodermal morphogenesis and F-actin dynamics for neural tube closure. Significantly, the *Drosophila* homologue *Grainyhead* (*grh*) is required for dorsal closure that is an analog event of neural tube closure and wound healing in vertebrates [37], suggesting an evolutionally conserved role of Grhl transcription factors in epithelial closure processes, with potentially varied cellular mechanisms among different anatomical regions and species.

Supplementary Material

Refer to Web version on PubMed Central for supplementary material.

Acknowledgments

We are grateful to Jose Munoz & Payman Mosaffa (Universitat Politècnica de Catalunya), Yanlan Mao (University of College London), and Priyom Adhyapok & James Glazier (Indiana University) for their collaborative efforts on computational simulation of the closure model in the past years; Alex Mogilner (New York University) and Edwin

Munro (Chicago University) for their discussion on the closure model; Pat Kysar (UC Davis) for technical advice on processing scanning electron microscopy; Lee Niswander (University of Colorado), Gabriel Galea & Andrew Copp (University of College London), Kate McDole & Keller Philipp and the Advanced Imaging Center (HHMI Janelia research campus) for their discussion and consideration of live imaging collaborations on the closure model. This work was supported by grants from the NIH (R01NS102261, R01DE026737 & R01DE0221696 to C. Z.) and the Shriners Hospitals for Children (86600 & 85105 to C.Z.).

References

[1]. Greene ND, Copp AJ, Development of the vertebrate central nervous system: formation of the neural tube, Prenat Diagn 29 (2009) 303–311. 10.1002/pd.2206. [PubMed: 19206138]

[2]. Wilde JJ, Petersen JR, Niswander L, Genetic, epigenetic, and environmental contributions to neural tube closure, Annu Rev Genet 48 (2014) 583–611. 10.1146/annurev-genet-120213-092208. [PubMed: 25292356]

[3]. Wallingford JB, Niswander LA, Shaw GM, Finnell RH, The continuing challenge of understanding, preventing, and treating neural tube defects, Science 339 (2013) 1222002 10.1126/science.1222002. [PubMed: 23449594]

[4]. Copp AJ, Stanier P, Greene ND, Neural tube defects: recent advances, unsolved questions, and controversies, Lancet Neurol 12 (2013) 799–810. 10.1016/S1474-4422(13)70110-8. [PubMed: 23790957]

[5]. Greene ND, Stanier P, Copp AJ, Genetics of human neural tube defects, Hum Mol Genet 18 (2009) R113–129. 10.1093/hmg/ddp347. [PubMed: 19808787]

[6]. Botto LD, Moore CA, Khoury MJ, Erickson JD, Neural-tube defects N Engl J Med 341 (1999) 1509–1519. [PubMed: 10559453]

[7]. Copp AJ, Adzick NS, Chitty LS, Fletcher JM, Holmbeck GN, Shaw GM, Spina bifida, Nat Rev Dis Primers 1 (2015) 15007 10.1038/nrdp.2015.7. [PubMed: 27189655]

[8]. Mitchell LE, Adzick NS, Melchionne J, Pasquariello PS, Sutton LN, Whitehead AS, Spina bifida, Lancet 364 (2004) 1885–1895. [PubMed: 15555669]

[9]. Harris MJ, Juriloff DM, Genetic landmarks for defects in mouse neural tube closure, Teratology 56 (1997) 177–187. [PubMed: 9358605]

[10]. Juriloff DM, Harris MJ, Mouse models for neural tube closure defects, Hum Mol Genet 9 (2000) 993–1000. [PubMed: 10767323]

[11]. Harris MJ, Juriloff DM, Mouse mutants with neural tube closure defects and their role in understanding human neural tube defects, Birth Defects Res A Clin Mol Teratol 79 (2007) 187–210. 10.1002/bdra.20333. [PubMed: 17177317]

[12]. Harris MJ, Juriloff DM, An update to the list of mouse mutants with neural tube closure defects and advances toward a complete genetic perspective of neural tube closure, Birth Defects Res A Clin Mol Teratol 88 (2010) 653–669. 10.1002/bdra.20676. [PubMed: 20740593]

[13]. Greene ND, Copp AJ, Mouse models of neural tube defects: investigating preventive mechanisms, Am J Med Genet C Semin Med Genet 135 (2005) 31–41.

[14]. Leduc RY, Singh P, McDermid HE, Genetic backgrounds and modifier genes of NTD mouse models: An opportunity for greater understanding of the multifactorial etiology of neural tube defects, Birth Defects Res 109 (2017) 140–152. 10.1002/bdra.23554. [PubMed: 27768235]

[15]. Martin AC, Goldstein B, Apical constriction: themes and variations on a cellular mechanism driving morphogenesis, Development 141 (2014) 1987–1998. 10.1242/dev.102228. [PubMed: 24803648]

[16]. Nikolopoulou E, Galea GL, Rolo A, Greene ND, Copp AJ, Neural tube closure: cellular, molecular and biomechanical mechanisms, Development 144 (2017) 552–566. 10.1242/dev.145904. [PubMed: 28196803]

[17]. Eom DS, Amarnath S, Agarwala S, Apicobasal polarity and neural tube closure, Dev Growth Differ 55 (2013) 164–172. 10.1111/dgd.12030. [PubMed: 23277919]

[18]. Waterman RE, Topographical changes along the neural fold associated with neurulation in the hamster and mouse, Am J Anat 146 (1976) 151–171. 10.1002/aja.1001460204. [PubMed: 941847]

[19]. Geelen JA, Langman J, Ultrastructural observations on closure of the neural tube in the mouse, Anat Embryol (Berl) 156 (1979) 73–88. 10.1007/bf00315716. [PubMed: 453553]

[20]. Rolo A, Savery D, Escuin S, de Castro SC, Armer HE, Munro PM, Mole MA, Greene ND, Copp AJ, Regulation of cell protrusions by small GTPases during fusion of the neural folds, Elife 5 (2016) e13273 10.7554/eLife.13273. [PubMed: 27114066]

[21]. Camerer E, Barker A, Duong DN, Ganesan R, Kataoka H, Cornelissen I, Darragh MR, Hussain A, Zheng YW, Srinivasan Y, Brown C, Xu SM, Regard JB, Lin CY, Craik CS, Kirchhofer D, Coughlin SR, Local protease signaling contributes to neural tube closure in the mouse embryo, Dev Cell 18 (2010) 25–38. 10.1016/j.devcel.2009.11.014. [PubMed: 20152175]

[22]. Muzumdar MD, Tasic B, Miyamichi K, Li L, Luo L, A global double-fluorescent Cre reporter mouse, Genesis 45 (2007) 593–605. 10.1002/dvg.20335. [PubMed: 17868096]

[23]. Song L, Li Y, Wang K, Wang YZ, Molotkov A, Gao L, Zhao T, Yamagami T, Wang Y, Gan Q, Pleasure DE, Zhou CJ, Lrp6-mediated canonical Wnt signaling is required for lip formation and fusion, Development 136 (2009) 3161–3171. 10.1242/dev.037440. [PubMed: 19700620]

[24]. Ting SB, Wilanowski T, Auden A, Hall M, Voss AK, Thomas T, Parekh V, Cunningham JM, Jane SM, Inositol- and folate-resistant neural tube defects in mice lacking the epithelial-specific factor Grhl-3, Nat Med 9 (2003) 1513–1519. [PubMed: 14608380]

[25]. Lemay P, De Marco P, Emond A, Spiegelman D, Dionne-Laporte A, Laurent S, Merello E, Accogli A, Rouleau GA, Capra V, Kibar Z, Rare deleterious variants in GRHL3 are associated with human spina bifida, Hum Mutat 38 (2017) 716–724. 10.1002/humu.23214. [PubMed: 28276201]

[26]. Rifat Y, Parekh V, Wilanowski T, Hislop NR, Auden A, Ting SB, Cunningham JM, Jane SM, Regional neural tube closure defined by the Grainy head-like transcription factors, Dev Biol 345 (2010) 237–245. 10.1016/j.ydbio.2010.07.017. [PubMed: 20654612]

[27]. Gustavsson P, Greene ND, Lad D, Pauws E, de Castro SC, Stanier P, Copp AJ, Increased expression of Grainyhead-like-3 rescues spina bifida in a folate-resistant mouse model, Hum Mol Genet 16 (2007) 2640–2646. 10.1093/hmg/ddm221. [PubMed: 17720888]

[28]. Galea GL, Cho YJ, Galea G, Mole MA, Rolo A, Savery D, Moulding D, Culshaw LH, Nikolopoulou E, Greene NDE, Copp AJ, Biomechanical coupling facilitates spinal neural tube closure in mouse embryos, Proc Natl Acad Sci U S A 114 (2017) E5177–E5186. 10.1073/pnas.1700934114. [PubMed: 28607062]

[29]. Pyrgaki C, Trainor P, Hadjantonakis AK, Niswander L, Dynamic imaging of mammalian neural tube closure, Dev Biol 344 (2010) 941–947. 10.1016/j.ydbio.2010.06.010. [PubMed: 20558153]

[30]. Massarwa R, Ray HJ, Niswander L, Morphogenetic movements in the neural plate and neural tube: mouse, Wiley Interdiscip Rev Dev Biol 3 (2014) 59–68. 10.1002/wdev.120. [PubMed: 24902834]

[31]. Massarwa R, Niswander L, In toto live imaging of mouse morphogenesis and new insights into neural tube closure, Development 140 (2013) 226–236. 10.1242/dev.085001. [PubMed: 23175632]

[32]. Ray HJ, Niswander LA, Dynamic behaviors of the non-neural ectoderm during mammalian cranial neural tube closure, Dev Biol 416 (2016) 279–285. 10.1016/j.ydbio.2016.06.030. [PubMed: 27343896]

[33]. De Castro SC, Leung KY, Savery D, Burren K, Rozen R, Copp AJ, Greene ND, Neural tube defects induced by folate deficiency in mutant curly tail (Grhl3) embryos are associated with alteration in folate one-carbon metabolism but are unlikely to result from diminished methylation, Birth Defects Res A Clin Mol Teratol 88 (2010) 612–618. 10.1002/bdra.20690. [PubMed: 20589880]

[34]. De Castro SCP, Gustavsson P, Marshall AR, Gordon WM, Galea G, Nikolopoulou E, Savery D, Rolo A, Stanier P, Andersen B, Copp AJ, Greene NDE, Overexpression of Grainyhead-like 3 causes spina bifida and interacts genetically with mutant alleles of Grhl2 and Vangl2 in mice, Hum Mol Genet 27 (2018) 4218–4230. 10.1093/hmg/ddy313. [PubMed: 30189017]

[35]. Zhao T, Gan Q, Stokes A, Lassiter RN, Wang Y, Chan J, Han JX, Pleasure DE, Epstein JA, Zhou CJ, beta-catenin regulates Pax3 and Cdx2 for caudal neural tube closure and elongation, Development 141 (2014) 148–157. 10.1242/dev.101550. [PubMed: 24284205]

[36]. Kimura-Yoshida C, Mochida K, Ellwanger K, Niehrs C, Matsuo I, Fate Specification of Neural Plate Border by Canonical Wnt Signaling and Grhl3 is Crucial for Neural Tube Closure, EBioMedicine 2 (2015) 513–527. 10.1016/j.ebiom.2015.04.012. [PubMed: 26288816]

[37]. Attardi LD, Von Seggern D, Tjian R, Ectopic expression of wild-type or a dominant-negative mutant of transcription factor NTF-1 disrupts normal Drosophila development, Proc Natl Acad Sci U S A 90 (1993) 10563–10567. 10.1073/pnas.90.22.10563. [PubMed: 8248145]

Highlights

- Non-neural ectodermal cells form multicellular rosettes during mouse PNP closure
- Rosette-forming cells generate convergent F-actin protrusions and cable network
- Rosettes and protrusions are disrupted in the surface ectodermal Grhl3-KO mutants
- Computational modeling visualizes the stepwise closure of mouse PNP

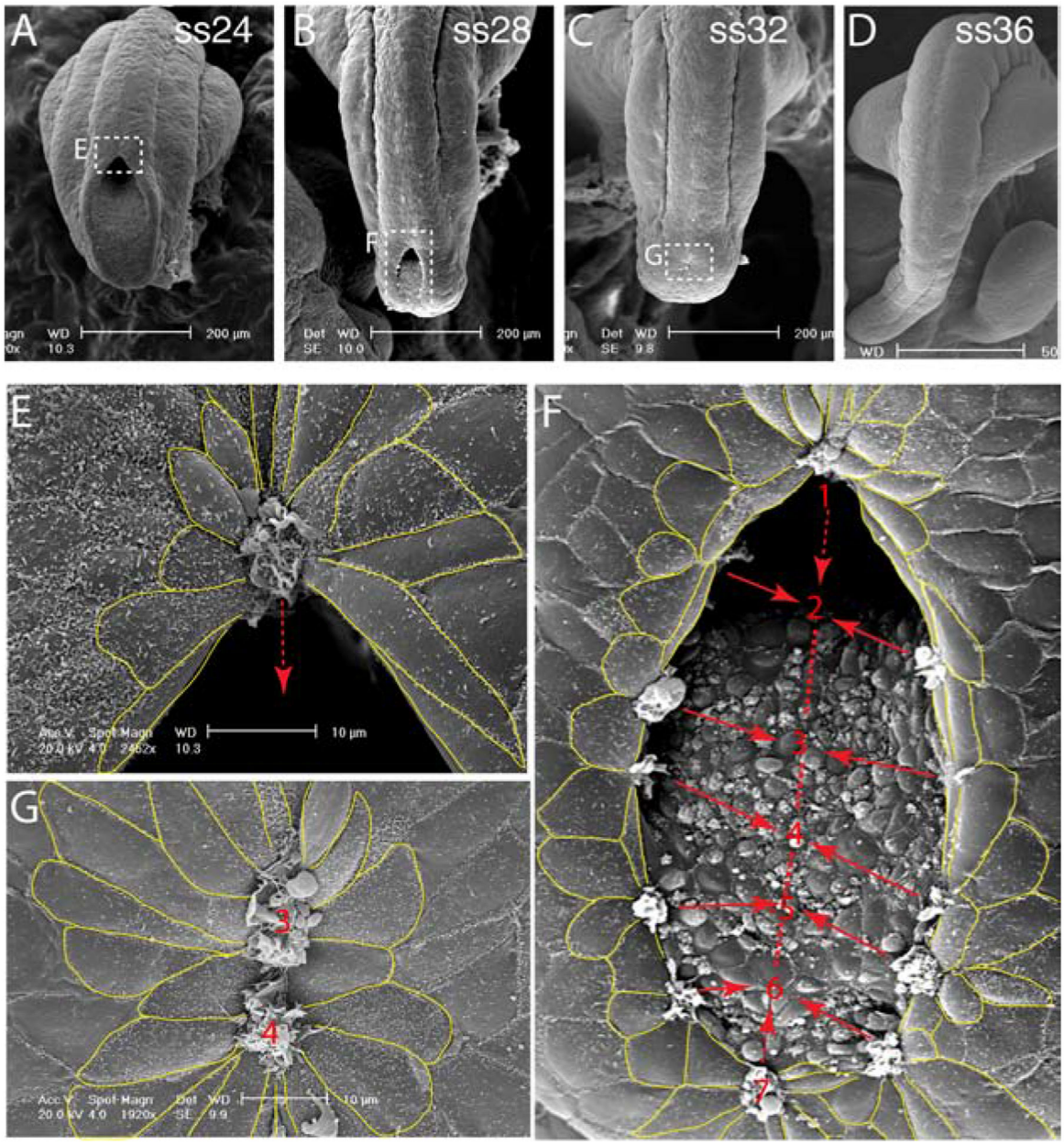

Fig. 1.

Surface ectodermal rosette formation and convergent cellular protrusions during the normal closure of the posterior neural pore (PNP) in the wild-type mouse embryos. (A-D) Dorsal views of the caudal mouse embryos with a large ongoing PNP closure site at E9.5 around ss24 (A), a late closure site at ss28 (B), the final fusion site at ss32 (C), and a completely closed neural tube at E10.5 around ss36 (D). (E) Enlarged view of the dashed rectangle in A clearly shows a forming rosette of the surface ectodermal cells with convergent cellular protrusions at the fusion site. Dashed arrow indicates the closure direction towards the posterior end of the neural fold. (F) Enlarged view of the dashed rectangle in B demonstrates a late closure site with the last seven paired rosette formation, including two midline rosettes/protrusions located at the leading fusion sites (1 and 7) and five paired partial

rosettes/protrusions (2 to 6) towards the midline fusion sites. (G) Enlarged view of the dashed rectangle in C demonstrates the final fusion site with the last two merged rosettes and convergent protrusions that are approximately equivalent to the rosette fusion sites of 3 and 4 in F. ss, somite stage.

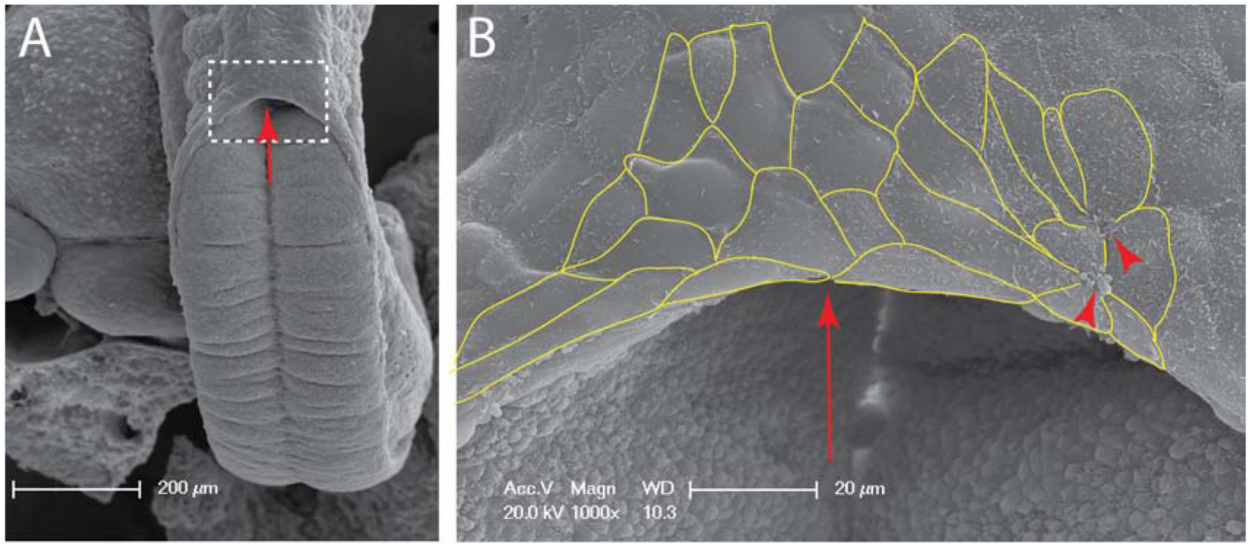

Fig. 2.

Disrupted rosette formation and convergent protrusions with defective PNP closure in the surface ectoderm mutant mouse embryo at E9.5. The midline rosette formation and cellular protrusions as seen in the normal control embryo (A) are severely disrupted in the defective PNPs of *Grhl3-KO* mouse embryo. The dashed rectangles in A is enlarged in B. *Arrows* indicate the defective leading fusion site by missing the midline rosette and protrusions. *Arrowheads* indicate the relocated rosette protrusions away from the closure sites (B).

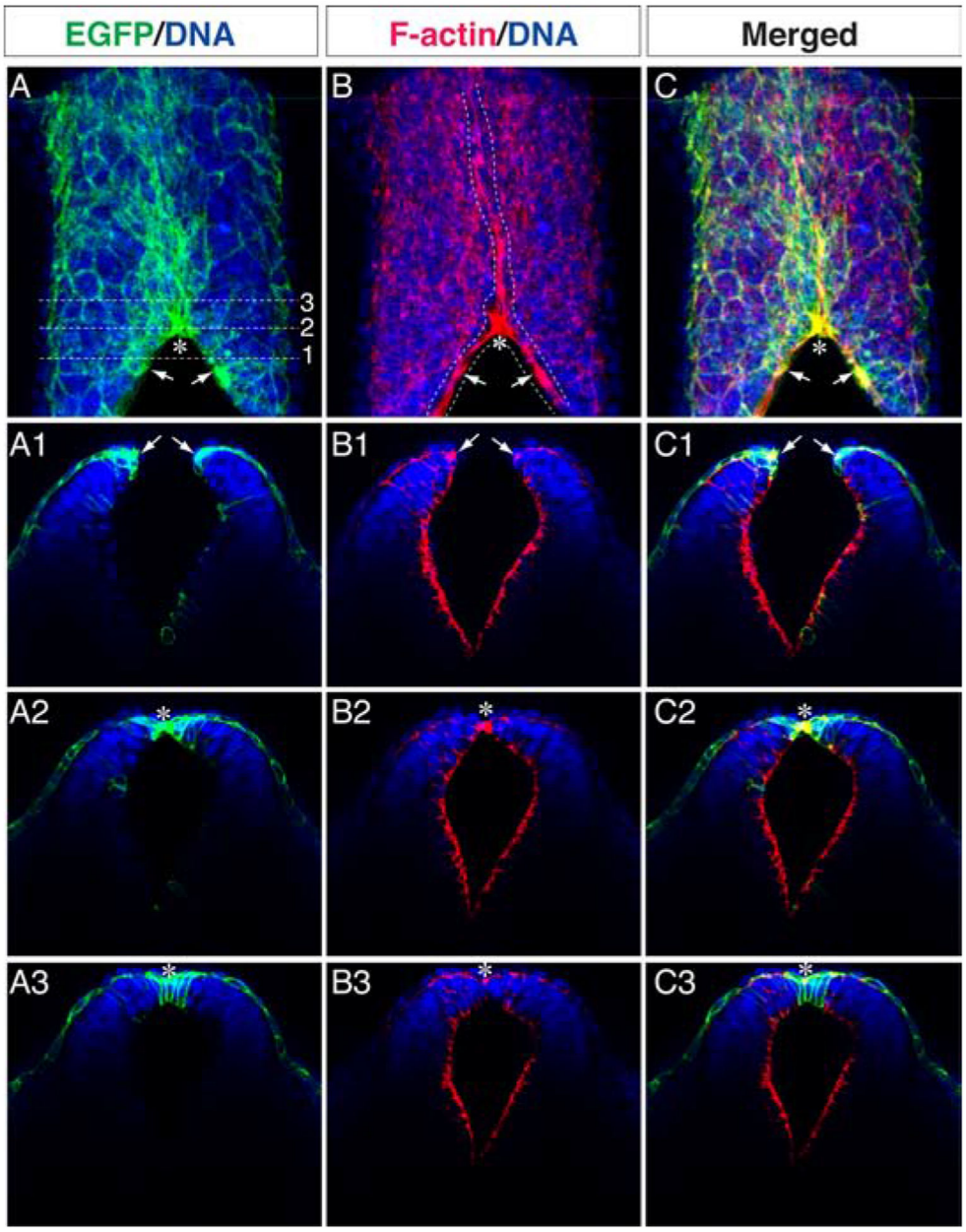

Fig. 3.

Genetic fate mapping and F-actin labeling demonstrate an F-actin protrusion and cable network generated by the rosette-forming surface ectodermal cells during PNP closure. (A-C) Dorsal views of the PNP by co-labeling of the genetically fate-mapped Grhl3^{Cre};EGFP positive surface ectodermal cells (*green*) and phalloidin-labeled F-actin (*red*). *Dashed lines* in B indicate the F-actin cables running through the closed midline (*top*), the leading fusion site (*asterisk*), and both edges of the pending closure sites (*arrows*). (A1-C3) Transverse sections of the pending closing (A1-C1), leading fusion (A2-C2), and post-fusion (A3-C3) sites, corresponding to the dashed lines in A.

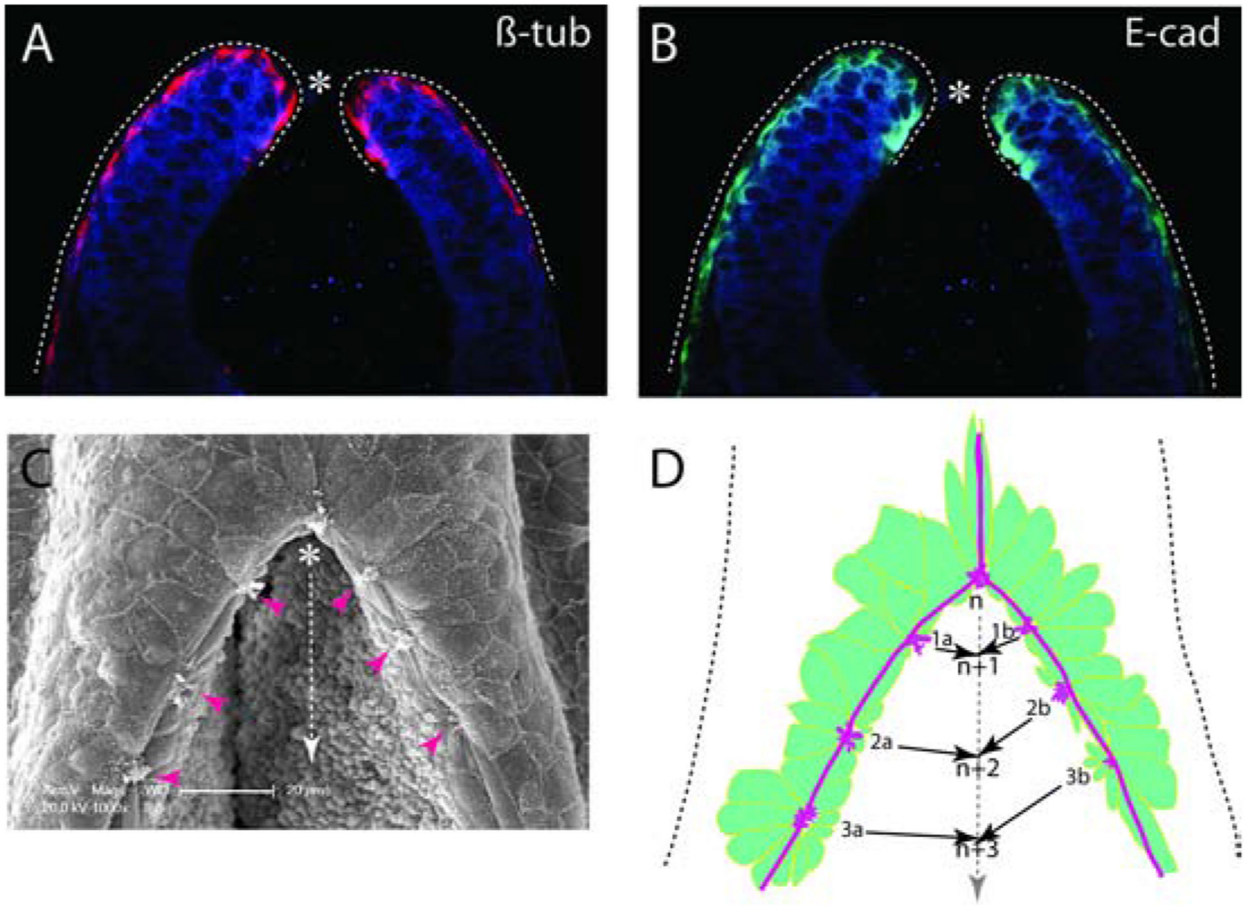

Fig. 4.

Immunolabeling of surface ectodermal markers endorses a novel model of PNP closure. (A,B) Immunofluorescence for ß-tubulin and E-cadherin on a transverse section of E9.5 mouse PNP demonstrating a single layer of the surface ectodermal cells (*dashed lines*) which extend into the inner side of the dorsal PNP, and wrap up the dorsal tips where they meet and fuse at the midline (*asterisk*). (C) A SEM micrograph of E9.5 PNP showing a midline rosette and its convergent protrusion cluster at the leading fusion site (*asterisk*), three adjacent rosettes and their respective protrusions (*arrowheads*) on each side of the pending closure PNP. (D) A mechanistic model for PNP closure driven by surface ectodermal rosette formation and F-actin protrusion/cable network. The convergent F-actin protrusions from the rosette-forming cells generate the force to tighten the F-actin cables and to pull the paired rosettes toward the midline. When the paired rosette protrusions of “1a” and “1b” meet at the midline and fuse at “n1”, a transiently existing full rosette “n” will form at the midline, resulting in one-cell length closure from “n” to “n+1”. Sequentially, it will start the next full rosette formation of “n+1” when the next paired rosettes meet at “n +2”, and so on, advancing the PNP closure. *Dashed arrow* indicates the closure direction towards the tailbud.